Journal of Power Sources 198 (2012) 294–297

Contents lists available at SciVerse ScienceDirect

Journal of Power Sources

journal homepage: www.elsevier.com/locate/jpowsour

Synthesis of entanglement structure in nanosized $Li_4Ti_5O_{12}$/multi-walled carbon nanotubes composite anode material for Li-ion batteries by ball-milling-assisted solid-state reaction

Yi Ruei Jhan, Jenq Gong Duh*

Department of Material Science and Engineering, National Tsing Hua University, Hsinchu, Taiwan

ARTICLE INFO

Article history:
Received 12 July 2011
Received in revised form 7 September 2011
Accepted 21 September 2011
Available online 29 September 2011

Keywords:
Lithium titanate
Carbon nanotube
High rate capability
Lithium-ion battery
Anode materials

ABSTRACT

Solid-state reactions are used for synthesizing $Li_4Ti_5O_{12}$ (LTO) of high purity and crystallinity. However, it is not easy to control the particle size of LTO in these reactions. In this study, an entanglement structure for an LTO/multi-walled carbon nanotube (MWCNT) composite is prepared by a ball-milling-assisted solid-state reaction. The LTO nanoparticles are confined in the interspace of the MWCNT matrix via this architecture control. The additive of MWCNTs can prevent the aggregation of LTO particles during the calcination process of the solid-state reaction. In addition, the entanglement of the MWCNTs and LTO creates an effective conductive network, which improves the conductivity of LTO. Therefore, the entanglement structure improves the electrochemical properties of LTO, such as the rate capability and cycle performance.

1. Introduction

Lithium-ion batteries have been widely used as the main power source in consumer electronic devices. In recent years, the issue of global warming has made it essential to develop lithium-ion batteries that have high energy density and can deliver a large amount of power, which are a requirement for power sources used in electric vehicles and energy storage systems. Safety issues and cycling stability have become the main area of focus for the development of large-scale lithium-ion batteries.

Among the electrode materials that have been studied, $Li_4Ti_5O_{12}$ (LTO) is a promising material for the anode in lithium-ion batteries because it has excellent Li-ion insertion/extraction properties and the change in volume during the charge–discharge process is almost negligible; therefore, LTO has a reliable cycle performance. Moreover, this material has a lithium insertion plateau at 1.55 V (vs. Li/Li^+) because of which the deposition of metallic lithium and decomposition of the electrolyte are prevented. Therefore, the degree of safety offered by lithium-ion batteries is expected to improve considerably. However, the insulating property of LTO arising from the empty Ti 3d state results in poor rate capability and thus prevents it from being widely used.

Various approaches have been studied for improving the electrical conductivity of LTO, such as decreasing the particle size of the material via advanced synthesis techniques to reduce the Li^+ diffusion path [1–3]. An alternative approach is to apply a coating of conductive materials on the surface of LTO [4,5].

However, nanoparticles have a tendency to attract each other, which results in an increase in the interparticle contact resistance; this in turn limits the electronic conduction path to the current collector [6,7]. In addition, it is rather difficult to achieve a uniform surface coating around the entire LTO particle. Therefore, a hybrid nanostructure electrode, in which particle growth can be controlled and which has a conductive additive nanophase, is an ideal material for both rapid electronic and ionic transport, which are required for achieving good rate capability [8]. High-temperature heat treatment is essential for preparing pure, well-crystallized LTO powder. The fabrication of a nanosized LTO with a high dispersity is very difficult in conventional solid-state reaction processes [9–11] as well as in sol–gel processes [12–15]. Carbon nanotubes (CNTs) have been used in Sn-based anode materials for lithium-ion batteries because of their unique properties, which include a high length–diameter ratio, strength, and flexibility and unique conductivity [16–18].

In this study, a practical and efficient method for synthesizing an LTO/multi-walled carbon nanotubes (MWCNTs) hybrid composite was developed. The MWCNTs act as: (i) a separator that prevents the repeated aggregation of LTO nanoparticles during the calcination process and (ii) a support matrix to provide a 3D conductive network. By using this method, the LTO particle's size can

* Corresponding author. Tel.: +886 3 5712686; fax: +886 3 5712686.
E-mail address: jgd@mx.nthu.edu.tw (J.G. Duh).

0378-7753/$ – see front matter © 2011 Elsevier B.V. All rights reserved.
doi:10.1016/j.jpowsour.2011.09.063

be restricted to approximately 100 nm. In addition, the LTO particles and MWCNTs are in close contact with each other. The hybrid composite having an entanglement structure of LTO/MWCNTs combines the advantages of both nanosized particles and a conductive adhesion to improve the electrochemical performance of LTO. The LTO/MWCNTs electrode allows for a good lithium insertion/extraction performance at a high rate capability and provides a good cycle performance.

2. Experimental

The LTO/MWCNTs composite was prepared by a solid-state reaction using LiCl, $H_2C_2O_4$, $TiCl_4$, and MWCNTs as the raw materials. First, an appropriate amount of LiCl and 70 wt% of $H_2C_2O_4$ was mixed together, and then, $TiCl_4$ was added. The precursor was heated at 150 °C for 0.5 h. Next, the precursor was sintered at 400 °C for 3 h in air. After sintering, the as-prepared powder was prepared by ball milling the sintered precursor with 5 wt% of MWCNTs in ethanol for 12 h and then drying at 100 °C for 12 h. Finally, the well-dispersed Li_2O–TiO_2/MWCNTs powder was calcined at 800 °C for 10 h in an atmosphere of Ar/H_2 mixed in the ratio of 93:7. To study the effect of the addition of MWCNTs to LTO, a sample without the addition of MWCNTs was also prepared by a similar process. The crystal structure of the as-prepared anode material was studied by X-ray diffraction (XRD) (Rigaku, D/MAX-B, Japan) using Cu Kα radiation at 30 kV and 20 mA. The surface morphology of this powder was examined using a field emission scanning electron microscope (FE-7600, JEOL). TEM images were taken using a JEOL JSM-2010 operated at 200 kV.

Electrochemical measurements were performed using R2032 coin cells. The anodes were made of either pristine LTO and LTO/MWCNTs active materials, a carbon black conductive agent, and a polyvinylidene fluoride binder; the materials were mixed in the ratio of 80:13:7. These materials were thoroughly mixed in N-methyl-2-pyrrolidinone solution. The prepared slurry was then coated with Cu foil. The electrolyte solution was 1 M $LiPF_6$ in ethylene carbonate–diethyl carbonate (1:1 vol%). Electrical impedance spectroscopy experiments were performed using a Parstat 2273.

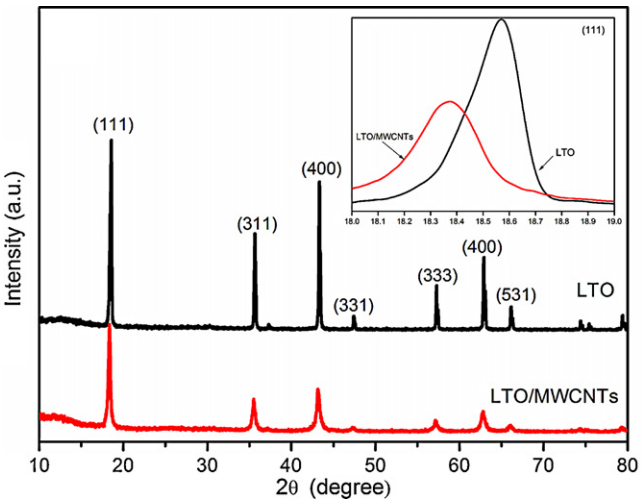

Fig. 1. XRD patterns of LTO and LTO/MWCNTs composite material.

3. Results and discussion

Fig. 1 shows the XRD patterns of the as-prepared pristine LTO and LTO/MWCNTs composite. The diffraction peaks of all the samples are indexed as a cubic spinel LTO phase. The absence of impurities in LTO, as observed from the XRD pattern, indicates that the absence of the MWCNTs around the LTO nanoparticles is most likely due to the very low content or amorphous carbon. The main diffraction peaks of the LTO/MWCNTs composite are

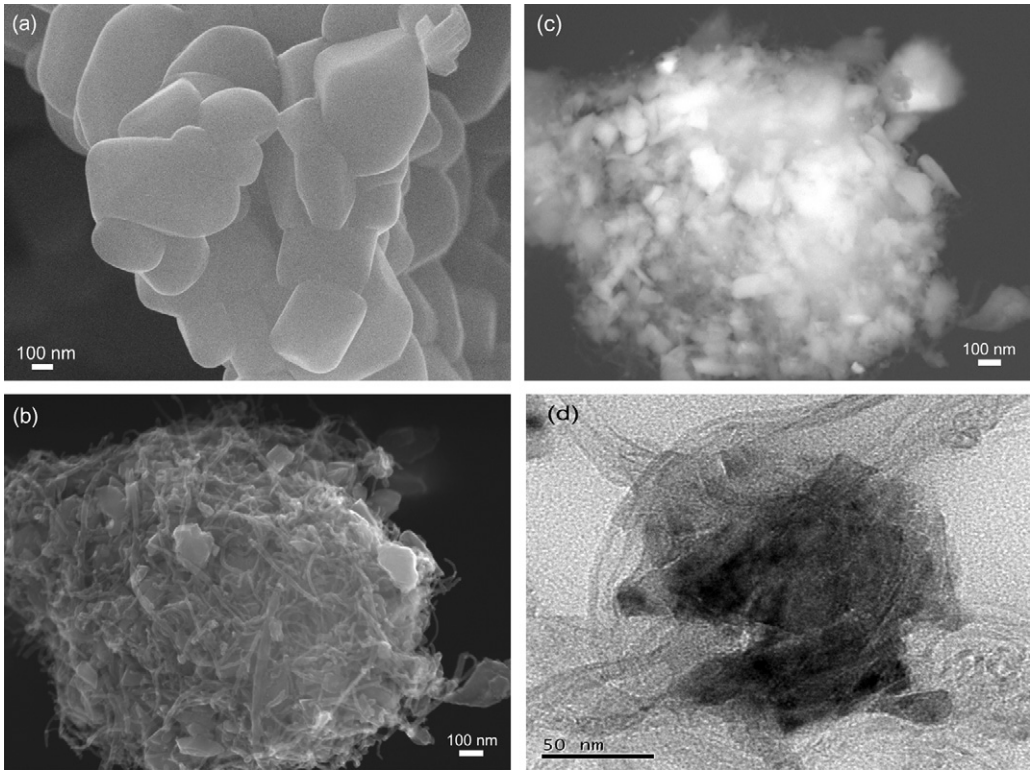

Fig. 2. SEM image of: (a) pristine LTO; (b) LTO/MWCNTs composite material; (c) BEI image of LTO/MWCNTs composite material and (d) TEM image of LTO/MWCNTs composite material.

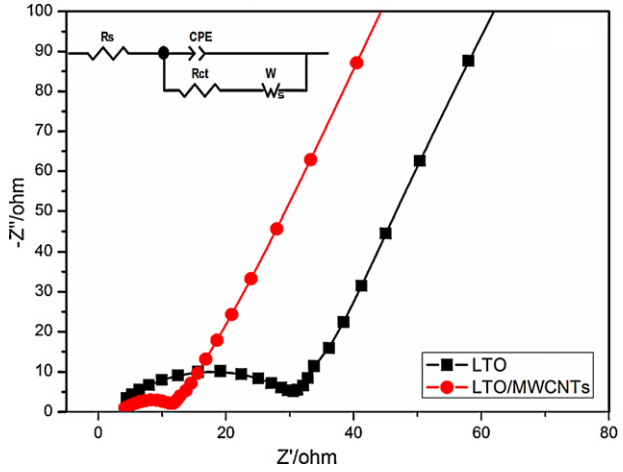

Fig. 3. AC impedance spectra of pristine LTO and LTO/MWCNTs.

somewhat broadened and the relative peak intensity is much lesser than that of the pristine LTO. This difference can be ascribed to the small particle size of the LTO/MWCNTs composite. In addition, a slight shift in the diffraction to a lower value of 2θ was observed for the LTO/MWCNTs composite (shown in the inset in Fig. 1). The lattice parameters of the pristine LTO and LTO/MWCNTs composite were calculated to be 8.348 and 8.369 Å, respectively. The lattice parameters for the LTO/MWCNTs composite are expected to be large if some of the Ti^{4+} ions transform to Ti^{3+} ions because of the larger ionic radius of Ti^{3+}, which is 0.67 Å as compared to the radius of Ti^{4+}, which is 0.61 Å [19,20]. This might improve the intrinsic electrical conductivity of LTO owing to the introduction of Ti^{3+}.

Some particles are aggregated into micron-sized particles. As seen in Fig. 2(b), only a few LTO particles appear in the secondary electron image, implying that only a small amount of LTO particles were dispersed on the surface of the entangled MWCNTs. However, the backscattered electron images, at the same position, revealed numerous bright areas and spots dispersed in the MWCNT matrix. These bright areas and spots represent the LTO nanoparticles (Fig. 2(c)). In the LTO/MWCNTs composite, most of the carbon nanotubes are entangled together, and the MWCNT web captures a majority of the LTO nanoparticles, which are 50–200 nm in diameter; this in turn prevents the aggregation of LTO nanoparticles. In addition, LTO particles were in close contact with the 3D conductive MWCNT matrix. The TEM image (Fig. 2(d)) shows the entanglement of the carbon nanotubes with the LTO particles, which effectively improves the electrical contact between the LTO particles and hence enhances the electrical conductivity of LTO.

Fig. 3 shows the diagrams of LTO and the LTO/MWCNTs composite. The tests were performed after the cells were charged/discharged for 1 cycle; they were measured at a stable voltage of 1.5 V. The AC impedance spectra are fitted with the help of an equivalent circuit (shown in the inset in Fig. 3). In the equivalent circuit, R_s and R_{ct} are the solution resistance and charge transfer resistance, respectively. A constant phase element is used to represent the double-layer capacitance and passivation-film capacitance, and W is the Warburg impedance. The parameters of the equivalent circuit and the exchange current densities ($i_0 = RT/nFR_{ct}$)

Table 1
Summary of AC-impedance parameters and electrochemical performance for the LTO and LTO/MWCNTs composite.

Sample	LTO	LTO/MWCNTs
R_s (Ω)	4.29	3.72
R_a (Ω)	31.77	9.66
i_0 (mA cm^{-2})	0.81	2.66

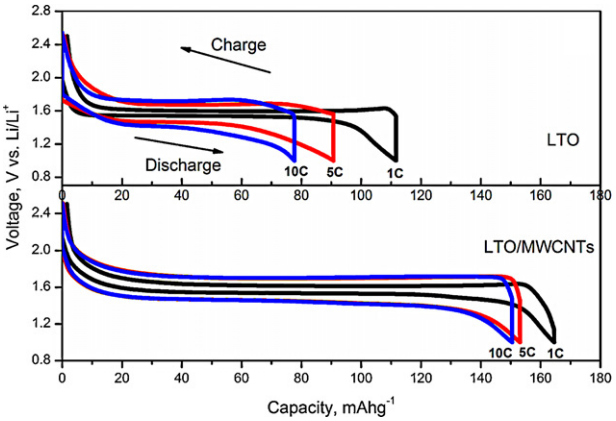

Fig. 4. The fifth charge/discharge curves of LTO and LTO/MWCNTs composite.

[21,22] are listed in Table 1. The LTO/MWCNTs composite exhibits a considerably lower impedance and a higher exchange current density than the pristine LTO. This improvement can be attributed to the interspace of the entangled MWCNTs, which act as a separator that prevents the aggregation of LTO nanoparticles during the calcination process, resulting in smaller-sized particles of LTO and in turn reducing the rate-limiting diffusion pathway in the LTO electrode material. The improvement can also be attributed to the insertion of the LTO particles into the MWCNT conductive matrix, which improves the contact between LTO particles and MWCNTs and hence assists electron transfer.

Fig. 4 shows the fifth charge/discharge of the pristine LTO and LTO/MWCNTs composite electrodes at various current rates of 1 C, 5 C, and 10 C. The capacity loss of the pristine LTO is 19% and 30% as the current rate increases from 1 C to 5 C and 1 C to 10 C, respectively. The severe loss in capacity is attributed to the large particle size of LTO, which induces a longer Li^+ diffusion path and poor electrical conductivity. Therefore, an electron and Li^+ cannot combine immediately. The accumulation of electrons and Li^+ ions results in polarization and causes a reduction in capacity. The voltage profiles of the LTO/MWCNTs electrodes reveal that the capacity loss is7% and 9% as the current rate increases from 1 C to 5 C and 1 C to 10 C, respectively. The substantial increase in the rate performance can be attributed to the entanglement structure that provides an excellent 3D conductive network and small-sized particles of LTO.

Fig. 5(a and b) shows the cycle performance of the pristine LTO and the LTO/MWCNTs composite electrodes as a function of the cycle number at current rates of 1 C, 5 C, and 10 C. The discharge capacity gradually decreases as the rate increases for all the samples. However, the LTO/MWCNTs composite electrode has a higher discharge capacity than the pristine LTO electrode. The initial discharge capacity of the LTO/MWCNTs composite

Table 2
Summarization electrochemical performance for the LTO and LTO/MWCNTs composite.

Sample	LTO			LTO/MWCNTs		
Charge–discharge rate	1 C	5 C	10 C	1 C	5 C	10 C
Discharge capacity at 100th cycle (mA h g^{-1})	111	89	70	161	152	147
Capacity retention after 100 cycles (%)	93	86	79	99	98	97

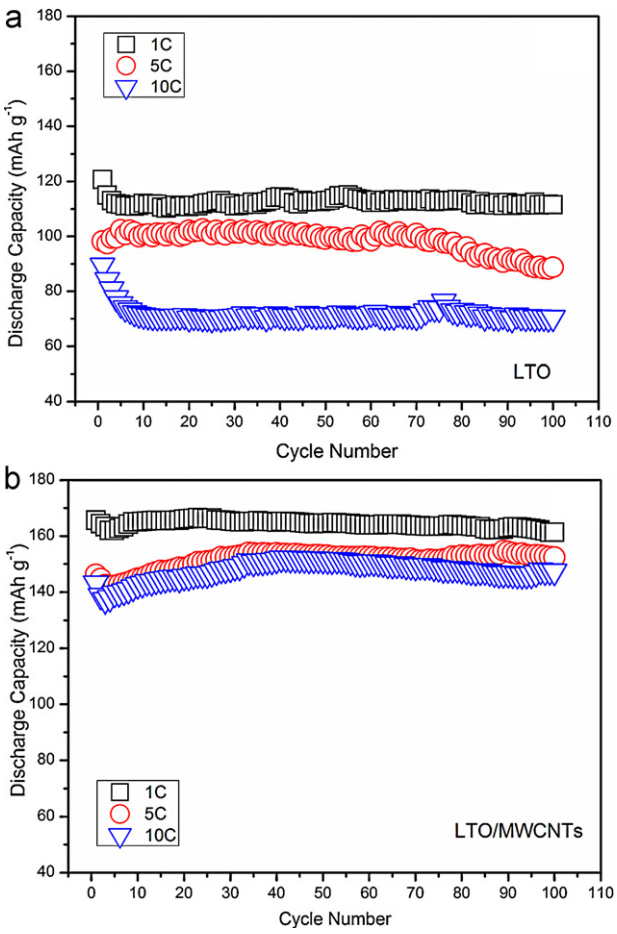

Fig. 5. Cycle performance curves of: (a) LTO and (b) LTO/MWCNTs composite electrodes at 1, 5 and 10 C rates.

electrode is 166 mA h g^{-1} at 1 C, and after 100 cycles, it is as high as 161 mA h g^{-1}.The electrode still maintains an excellent cycle performance although the current rate increases. The data of the electrochemical performance of the pristine LTO and LTO/MWCNTs electrodes are summarized in Table 2. This result indicates that the rate capability and cycle performance of a pristine LTO electrode can be effectively improved by the entanglement structure of the LTO/MWCNTs composite materials.

4. Conclusions

An LTO/MWCNTs composite having an entanglement structure was synthesized by the ball-milling-assisted solid-state reaction. The interspace of the MWCNT matrix effectively acts as the separator that prevents the aggregation of LTO nanoparticles during the calcination process. The conductive matrix is in close contact with the LTO nanoparticles. It is inferred that the short Li^+ diffusion path and closely contacted conductive network improve both the efficiency of the lithium ion and the electrical conductivity. After 100 cycles, at a current rate of 10 C, the discharge capacity is maintained at 147 mA h g^{-1}, which is 97% of the initial discharge capacity. Therefore, the LTO/MWCNTs composite with an entanglement structure is a reliable material for the anode of lithium-ion batteries; such batteries are expected to deliver high power and have a long cycle life.

Acknowledgements

This study was financially supported by National Science Council of Taiwan, under project no. NSC 96-2221-E-007-093-MY3 and from the Ministry of Economics under the project no. 98-EC-17-A-08-S1-003.

References

[1] G.J. Wang, J. Gao, L.J. Fu, N.H. Zhao, Y.P. Wu, T. Takamura, J. Power Sources 174 (2007) 1109.
[2] Y. Wang, H. Liu, K. Wang, H. Eiji, Y. Wang, H. Zhou Wang, J. Mater. Chem. 19 (2009) 6789.
[3] A. Guerfi, P. Charest, K. Kinoshita, M. Perrier, K. Zaghib, J. Power Sources 126 (2004) 163.
[4] L. Cheng, J. Yan, G.N. Zhu, J.Y. Luo, C.X. Wang, Y.Y. Xia, J. Mater. Chem. 20 (2010) 595.
[5] A.S. Prakash, P. Manikandan, K. Ramesha, M. Sathiya, J.M. Tarascon, A.K. Shukla, Chem. Mater. 22 (2010) 2857.
[6] R. Dominko, M. Gaberscek, M. Bele, D. Mihailovic, J. Jamnik, J. Eur. Ceram. Soc. 27 (2007) 909.
[7] I. Moriguchi, R. Hidaka, H. Yamada, T. Kudo, H. Murakami, N. Nakashima, Adv. Mater. 18 (2006) 69.
[8] L. Shen, C. Yuan, H. Luo, X. Zhang, S. Yanga, X. Lua, Nanoscale 3 (2001) 572.
[9] E. Ferg, R.J. Gummov, A. de Kock, M.M. Thacheray, J. Electrochem. Soc. 141 (1994) L147.
[10] T. Ohzuku, A. Ueda, N. Yamamoto, J. Electrochem. Soc. 142 (1995) 1431.
[11] K. Zighib, M. Simoneau, M. Armand, M. Gauthier, J. Power Sources 81–82 (1999) 300.
[12] S. Bach, J.P.P. Ramos, N. Baffier, J. Mater. Chem. 8 (1998) 251.
[13] M. Venkateswarlu, C.H. Chen, J.S. Do, C.W. Lin, T.C. Chou, B.J. Hwang, J. Power Sources 146 (2005) 204.
[14] C.M. Shen, X.G. Zhang, Y.K. Zhou, H.L. Li, Mater. Chem. Phys. 78 (2002) 437.
[15] Y.J. Hao, Q.Y. Lai, J.Z. Lu, H.L. Wang, Y.D. Chen, X.Y. Ji, J. Power Sources 158 (2006) 1358.
[16] Z.P. Guo, Z.W. Zhao, H.K. Liu, S.X. Dou, Carbon 43 (2005) 1392.
[17] J.H. Lee, B.S. Konga, S.B. Yanga, H.T. Jung, J. Power Sources 194 (2009) 520.
[18] Y.R Jhan, J.G. Duh, S.Y. Tsai, Diamond Relat. Mater. 20 (2011) 413.
[19] R.D. Shannon, Acta Crystallogr. Sect. A 32 (1976) 751.
[20] H.G. Jung, S.T. Myung, C.S. Yoon, S.B. Son, K.H. Oh, K. Amine, B. Scrosati, Y.K. Sun, Energy Environ. Sci. 4 (2011) 1345.
[21] A.Y. Shenouda, K.R. Murali, J. Power Sources 176 (2008) 332.
[22] A.Y. Shenouda, K. Hua, Liu, J. Alloys Compd. 477 (2009) 498.